

Biogenic Synthesis of Silver Nanoparticles Using *Citrus Limon* Leaves and Its Structural Investigation

Ravindra D. Kale and Priyanka Jagtap

1 Introduction

In the recent years, researchers have shown enormous positive attention for metal nanoparticles. These nanoparticles have wide range of applications in various diverse fields like pharmaceuticals, textiles, agriculture, cosmetics. The prevalent nanoparticle synthesis methods pose hazardous risks to the environment. Hence, a green route for biosynthesis of nanoparticles using the reducing phytochemicals from plant sources is emerging as a reliable and environment-friendly method.

Silver nanoparticles are widely used in many industries because of their efficient antimicrobial property. They find applications in textile finishing and effluent treatment. [1]. Various leaf extracts have been reported to give stable *n* crystalline silver nanoparticles viz. geranium leaf extract, *Azadirachta indica*, fruit extract of *Embalica officinalis* [2], aloe vera, *capsicum annum* [3, 4], *Helianthus annus*, *Basellaalba*, *Oryza sativa*, *Saccharum officinarum*, *Sorghum bicolor*, *Zea mays* [5], fruit extract of *Carica papaya* [6], Persimmon and Magnolia plants [7], *Jatropha curcas* [8], Eucalyptus hybrid leaves [9] and *Acalypha indica* leaf extract [10].

The present research work is undertaken to synthesize nano-sized silver particles using *Citrus Limon* leaves. Response surface methodology was used for the optimization of the production parameters. The nanoparticles were analysed for morphology, particle size and crystallinity.

R. D. Kale (✉) · P. Jagtap
Department of Fibres and Textile Processing Technology,
Institute of Chemical Technology, Mumbai 400019, India
e-mail: rd.kale@ictmumbai.edu.in

P. Jagtap
e-mail: jagtappu92@gmail.com

2 The Experiment

2.1 Materials

Fresh, dark green leaves of *Citrus Limon* were collected from the campus of Institute of Chemical Technology, Mumbai. Silver nitrate AgNO_3 (Mol. Wt. 169.70 g) salt, sodium hydroxide, sulphuric acid, Glauber's salt and soda ash were purchased from S. D. Fine-Chem Ltd. (SDFCL, Mumbai). C. I. Reactive Blue 171 was kindly provided by Atul Industries Limited, Mumbai. The other reagents were obtained from the laboratory and were of analytical grade.

2.2 Methods

Synthesis of Silver Nanoparticles

100 ml of silver nitrate solution with 0.01 M was prepared in an Erlenmeyer flask using distilled water. Fresh *Citrus Limon* leaves which were harvested from the on-campus plants were thoroughly washed with distilled water, finely chopped and added to the salt solution. The solution was continuously stirred on a shaker bath machine (Rossari Labtech, Mumbai) at 70 rpm. To study the effect of temperature, pH and amount of the leaves used as reducing agent various experiments were carried out according to the Design of Experiment for two hours. To maintain the pH, sulphuric acid 0.1 N and sodium hydroxide 0.1 N solutions were used. The formation of nanoparticles was evident from the colour change of the solution. After complete reduction of the silver nitrate, the solution was filtered and stored in colloidal form for further analysis and application.

Experimental Design for Optimization of Process Parameters

In this study, the possible effect of parameters like temperature, pH and amount of the reducing agent on silver nanoparticles synthesis was analysed and optimized using the response surface methodology. A central composite design (CCD) was obtained for the three factors at their high and low levels, and the centre and axial points were replicated. The experimental design consisted of 20 experimental runs which included eight cube points, six central points and six axial points. After each experimental run, absorbance at the maximum wavelength was measured spectrophotometrically indicating synthesis of nanoparticles.

Characterization of Silver Nanoparticles Synthesized Using Optimum Process Conditions

UV-Visible spectral analysis was done (UV-1800 ENG 240 V, Shimadzu) in the wavelengths ranging from 200–800 nm with a resolution of 1 nm. Laser diffraction technique was used for particle size analysis in terms of particle size and particle size distribution (SALD 7500 nano, Shimadzu, Japan). Transmission electron microscopy was used to study the morphological characteristics (TEM Model 200

Supertwin STEM (Phillips make)). X-ray diffraction analysis for the crystalline nature, quality and crystallographic determination of the silver nanoparticles was carried out using X-ray diffractometer (Shimadzu XRD-6100). The infrared spectra of the reducing agent and the silver nanoparticles were recorded on FTIR instrument (FTIR 8400S, Shimadzu, Japan) in the range of 4000–400 cm^{-1} . The chemical composition of the biosynthesized nanoparticles was examined in the Na–U channel using EDAX (EDX-720, Shimadzu). The optical examination of the original *Citrus Limon* leaves and after synthesizing nanoparticles was done using Leica DM EP microscope attached with a camera system Leica DMC 2900.

Decolourization of Textile Effluent with used *Citrus Limon* Leaves

The nanoparticle-deposited leaves were used to decolourize the textile effluent. C.I. Reactive Blue 171 effluent stock solution of 0.1 gpl was prepared. The leaves were put in this solution, and the solution was continuously stirred on a magnetic stirrer for 60 min at room temperature. After 60 min, the absorbance of the solution was measured on UV–Vis spectrophotometer at λ_{max} (620) nm and the percentage decolourization was calculated using Eq. 1.

$$\% \text{decolourization} = \frac{\text{Initial Concentration} - \text{Final Concentration}}{\text{Initial Concentration}} \times 100 \dots (1)$$

3 Results and Discussion

3.1 ANOVA Analysis

The results of the central composite design experimental runs are represented in Table 1. To calculate the optimal levels of the three process variables viz. temperature (A), pH (B) and amount of reducing agent (C), a second-order polynomial model was fit to determine the maximum nanoparticles synthesis and develop a relation between the response and the process variables. The maximum silver nanoparticles biosynthesis (absorbance 0.3725) was achieved in run six under the conditions of temperature 100 °C, pH 3 and 7.5 g of reducing agent.

$$\begin{aligned} \text{Absorbance} = & -0.40693 + 0.0189995 \times A - 0.0049525 \times B - 0.050922 \times C \\ & + 0.00005.85 \times A \times B + 0.000264 \times A \times C - 0.00003 \times B \\ & \times C - 0.00012904 \times (A)^2 - 0.0001875 \times (B)^2 \\ & + 0.00596 \times (C)^2 \dots \end{aligned} \quad (2)$$

After applying multiple regression analysis, the determination coefficient value of $R^2 = 0.91138$ was obtained. The high R^2 value indicates good correlation between the predicted and the observed values. Hence in the present study,

Table 1 CCD experimental run of trials with response for synthesis of silver nanoparticles using *Citrus Limon* leaves

Run	Temperature (°C)	pH	Amount of reducing agent	Absorbance at 410 nm	
				Experimental	Predicted
1	75	5	5	0.31	0.27731
2	75	5	5	0.2708	0.27731
3	75	5	5	0.2296	0.27731
4	75	5	5	0.2793	0.27731
5	75	3	5	0.2973	0.28174
6	100	3	7.5	0.3725	0.354285
7	75	5	5	0.2592	0.27731
8	100	3	2.5	0.1677	0.179345
9	50	7	2.5	0.117	0.139485
10	100	5	5	0.2079	0.22806
11	75	5	5	0.2808	0.27731
12	75	5	7.5	0.3574	0.38538
13	50	7	7.5	0.2552	0.247825
14	75	7	5	0.2729	0.27138
15	100	7	2.5	0.1786	0.175135
16	100	7	7.5	0.3596	0.349475
17	50	3	2.5	0.141	0.155395
18	75	5	2.5	0.2888	0.24374
19	50	5	5	0.2025	0.16526
20	50	3	7.5	0.2566	0.264335

independent variables had 91.138% variability. Also, a highly significant model was fit which was indicated by the adjusted determination coefficient (Adj. $R^2_{\text{abs}} = 0.90401$). ANOVA was employed to test the significance and adequacy of the model. F-values and p-values showed the significance of each coefficient which are listed in Table 2. The degree of significance shows that the linear and quadratic effects of A (temperature), B (pH) and C (amount of reducing agent) are significant, suggesting that the product production rate will be significantly altered with slight variation in these parameters. The interaction between studied variables and their optimal levels were determined using the response surface curves (shown in Fig. 1). This was done by fixing one of the variables at optimum value and allowing the others to be varied. Figure 1a shows that the interactive effect of the factors A and B is not significant on the synthesis of silver nanoparticles. The effect of pH is not very significant. Figure 1b shows that there is gradual increase of the silver nanoparticles biosynthesis with increasing the levels of temperature and the amount of reducing agent. The maximum silver nanoparticles yield was obtained at high temperatures. Figure 1c shows that higher levels of reducing agent amounts support high silver nanoparticles yield. Lower levels of pH and higher levels of amount of reducing agent lead to higher yields of the nanoparticles. The experimental and predicted results were in good agreement with accuracy of more than 95.08%,

Table 2 Analysis of variance (ANOVA) for optimization of silver nanoparticles synthesis

Source	Sum of squares	df	Mean square	F-value	p-value Prob > F	Confidence level
Model	0.084162036	9	0.009351	9.359527	0.000833	99.9167
A-Temperature	0.0098596	1	0.00986	9.868235	0.010486	98.9514
B-pH	0.000268324	1	0.000268	0.268559	0.615572	38.4428
C-Amount of reducing agent	0.050154724	1	0.050155	50.19865	0.0000335	99.99665
AB	0.000068445	1	0.0000684	0.068505	0.798838	20.1162
AC	0.002178	1	0.002178	2.179907	0.170606	82.9394
BC	0.00000018	1	0.00000018	0.00018	0.989555	1.0445
A^2	0.017887162	1	0.017887	17.90283	0.001741	99.8259
B^2	0.00000154687	1	0.00000155	0.001548	0.969388	3.0612
C^2	0.003815797	1	0.003816	3.819139	0.079187	92.0813

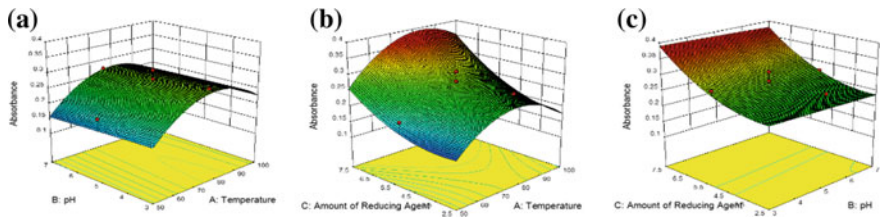


Fig. 1 3D response surface **a–c** showing the interactive effects of independent variables (temperature, pH and amount of reducing agent) on biosynthesis of silver nanoparticles using *Citrus Limon* leaves

thereby ensuring the validity of the model under the tested conditions. It was found that temperature of 95 °C, pH 3.2 and 7.5 g of reducing agent correspond to the optimal levels of the process variables for silver nanoparticles biosynthesis using *Citrus Limon* leaves.

3.2 Characterization of Silver Nanoparticles

The reduction of silver nitrate could be confirmed visually by observing the colour change of the solution, which changes colour from colourless to yellowish brown to reddish brown and finally to colloidal brown (Fig. 2a), indicating the formation of silver nanoparticles. The results are for biosynthesis of silver nanoparticles at 100 °C, pH 3 and with 7.5 g of reducing agent. It was observed that after 3 months of storage of the colloidal solution, the metal deposited on the inner surface of the storage container. This could be attributed to complete reduction of the metal into nanoparticles followed by agglomeration leading to conversion into metallic state.

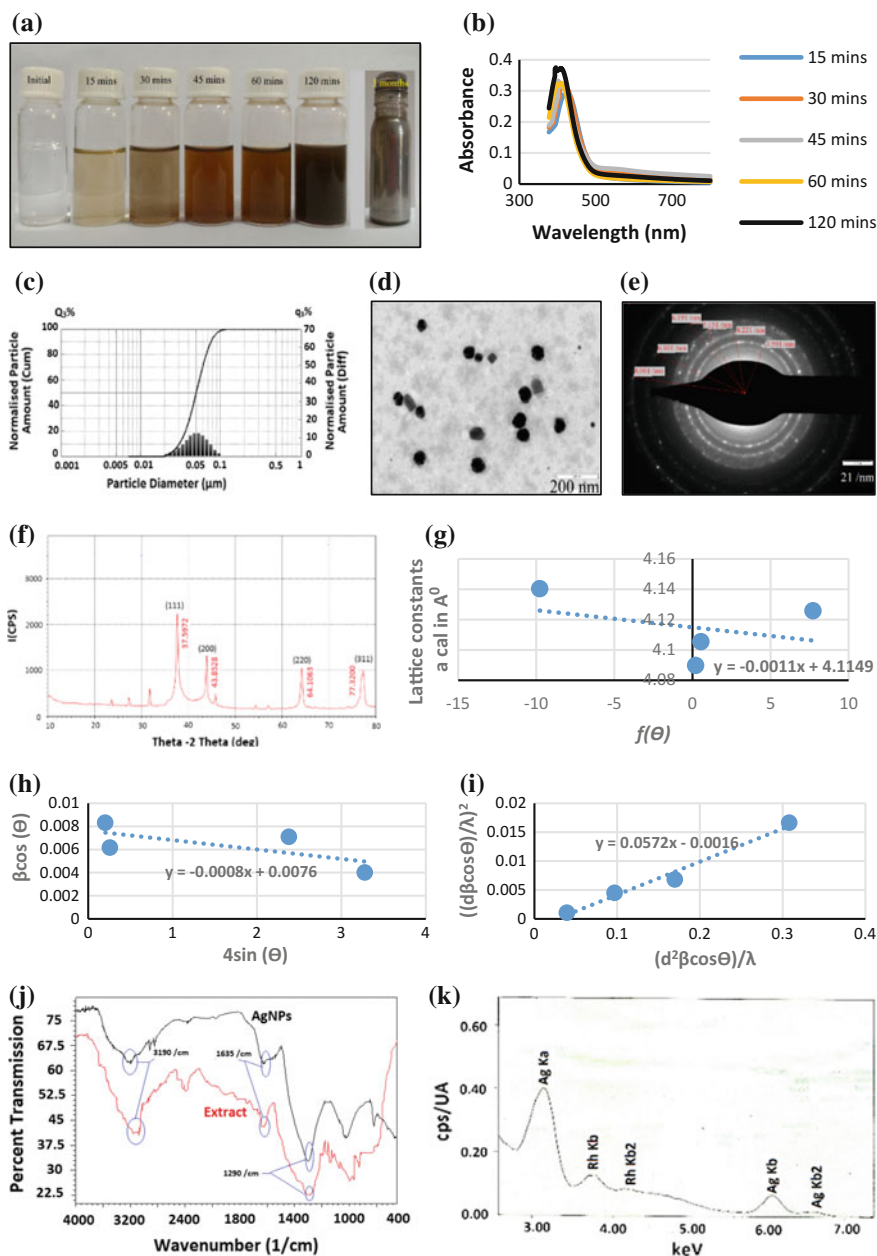


Fig. 2 **a** optical observation of Ag nanoparticles **b** UV-Vis absorption spectrum **c** particle size of biosynthesized Ag nanoparticles **d** TEM image **e** SAED pattern **f** XRD pattern **g** Nelson-Riley plot **h** uniform deformation model (W-H) plot **i** size-strain plot **j** FTIR spectrum **k** EDX pattern

This form can find many applications such as silver-coated bottles for milk feeds for babies, storage of cosmetics. The dispersed colloidal silver can find many applications such as preparation of cosmetics, bath soaps, disinfectants, agricultural uses. Also, it can find many applications in textile to improve the functionality of the textile substrate such as to impart conductivity to the textile substrate, antibacterial effect, magnetic properties, optical properties. The nanoparticles in powdered form can be used for the decolourization of the textile effluents.

Figure 2b shows the UV–Vis absorption spectrum of Ag nanoparticles suspension synthesized using *Citrus Limon* leaves as a function of reaction time. As reported in the earlier studies [10], the presence of absorbance peak in the region of 420–440 nm proves the formation of Ag nanoparticles. The other process conditions were fixed as 100 °C temperature, pH 3 and 7.5 g of *Citrus Limon* leaves. It was observed that the λ_{max} shifted from 425 to 422 nm with increasing reaction time from 15 to 30 min, and it centred at 422 nm for remaining samples.

Figure 2c shows the particle size distribution of the silver nanoparticles prepared by using *Citrus Limon* leaves. Silver nanoparticles with a mean particle size of 49 nm were obtained. The particle size analysis of the silver nanoparticles done by the laser diffraction technique shows median particle size of 49 nm, wherein 50% of the particles lie above 49 nm size and 50% of the particles lie below 49 nm size range. The modal particle size obtained by this analysis method was 56 nm, which represents the maximum value of the frequency distribution of the particles. 90% of the particles are below 76 nm size range, 50% of the particles are below 49 nm and 10% of the particles are below 30 nm range. The particles exhibit normal distribution with standard deviation of 0.153 nm which is significantly low. This shows the ability of the *Citrus Limon* leaves to act as a reducing agent in synthesizing Ag nanoparticles with narrow particle size distribution.

The morphology and size distribution of the synthesized silver nanoparticles were determined by TEM analysis. The TEM image in Fig. 2d shows that the particles were predominantly spherical with some particles of ellipsoidal shape. It also suggests that the particles ranged in size from 10 to 50 nm with an average diameter of 28 nm. The Ag particles were crystalline, as can be seen from the selected area electron diffraction (SAED) pattern, Fig. 2e recorded from one of the nanoparticles in the aggregate. SAED spots correspond to the different crystallographic planes of elemental silver.

Figure 2f shows the XRD pattern of Ag nanoparticles. Four distinct peaks are observed at 37.5972°, 43.8528°, 64.1063° and 77.32° with (111), (200), (220) and (311) Miller indices, respectively. These peaks correspond to Joint Committee on Powder Diffraction Standards (JCPDS), silver file No. 04-0783. It showed crystallinity of 36.69% which is also evident from the sharpness of the (111) peak. As compared to the diffraction angle of the bulk value ($2\theta = 44.3$; JCPDS 04-0783), the (200) plane has modified marginally towards lower angle, leading to compressive stress in the various lattice crystals. Hence, these lead to dislocations of the crystals. The corrected lattice constant, average stress and dislocation density obtained were 0.41149 nm (Table 3; Fig. 2g), 0.795×10^9 , 0.298×10^{16} N/m², respectively. The peak narrowing is resulted from this residual stress which is

Table 3 Structural parameters of biosynthesized Ag nanoparticles using *Citrus Limon* leaves

Plane spacing d (nm)	Crystallographic planes hkl	Bragg's diffraction angle 2θ	Lattice constant a_{cal} (nm)	Lattice constant $a_{\text{corrected}}$ (nm)
0.239044	111	37.5972	0.4140364	0.41149
0.206285	200	43.8528	0.41257	
0.245146	220	64.1063	0.4105349	
0.123308	311	77.3200	0.4089664	

Table 4 Particle size of Ag nanoparticle synthesized using *Citrus Limon* leaves calculated by different methods

Crystallite size D in nm				
Debye–Scherrer formula	UDM method (W–H) plot	SSP plot	Laser diffraction method	TEM
18.39	19.054	20.192	49	28

annotated from the UDM (Fig. 2h) and SSP (Fig. 2i) models [11]. The calculated crystallite size by the various methods was in good agreement with those obtained with the TEM and laser diffraction method (Table 4).

FTIR measurements helped in identifying the phytochemicals acting as reducing and capping agents. Figure 2j represents the FTIR spectrum of the colloidal silver nanoparticles and the leaf extract. It shows peaks at 3190, 2914, 2846, 1635, 1298, 1031 and 817 cm^{-1} .

The peak at 1635 cm^{-1} is assigned to the amide I band of proteins released from the leaves which could possibly be the chlorophyll present in the leaves. During the degreening process, the chlorophyll is converted into number of tetrapyrroles which act as the reducing agent. The peaks 1290 and 1031 cm^{-1} contribute to –CN stretching which could be possibly from amino acids or amines. It is well known that leaf extract contains large amounts of terpenoids, flavonoids, alkaloids and steroids. EDX spectroscopy analysis confirmed the presence of elemental silver by the signals (Fig. 2k) obtained in the range of 3–4 keV which is the typical absorption range of metallic silver nano-crystallites [10].

The microscopic images of the *Citrus Limon* leaves are shown in Fig. 3a, b. Because of the in situ extraction and synthesis of the nanoparticles, deposition of silver nanoparticles on the *Citrus Limon* leaves is observed. Textile effluents comprise of different dyes which make essential the use of prevailing techniques as well as to look for new techniques that can decolourize the dye mixtures. Use of metal nanoparticles for the decolourization process has been an effective way in the recent techniques employed. Efficient decolourization of the textile effluent has been observed with the use of Ni and Fe nanoparticles [12, 13]. In the present work, decolourization was attempted using nanoparticle-deposited leaves which showed decolourization efficiency of 91.07% (Fig. 3c). This could possibly be attributed to

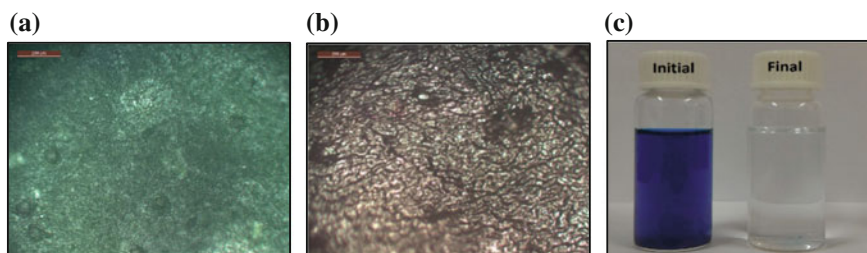


Fig. 3 **a** microscopic images of *Citrus Limon* leaves **b** microscopic images of *Citrus Limon* leaves after use for synthesis of Ag nanoparticles **c** decolourization of C.I. Reactive Blue 171 using silver nanoparticle-deposited *Citrus Limon* leaves

the nanoparticles deposited on the leaves which help in breakdown of the dye molecules. Hence, these leaves can be used for the decolourization of the textile effluent.

4 Conclusion

In conclusion, we are introducing an efficient environment-friendly biological procedure to synthesize silver nanoparticles using Citrus Limon leaves. Significant model was fit for the metal salts using the response surface methodology of Design of Experiment, and all the process parameters play a vital role in the nanoparticle synthesis. The particle size results for the nanoparticles were in good agreement with the results obtained by W–H plot and SSP method. XRD study revealed significant crystallinity of the nanoparticles. Spherical- to elliptical-shaped nanoparticles were obtained. Hence, it can be concluded that *Citrus Limon* leaves can be used for the synthesis of the well-dispersed nanoparticles without agglomeration. Also, the nanoparticle-deposited Citrus Limon leaves can be used in the decolouration of textile effluent which showed decolouration efficiency of 91.07%.

Acknowledgements Authors would like to acknowledge FIST–DST project, Govt. of India, and World Bank funded TEQIP-II for providing the machineries for this research project.

References

1. Jiang, H., Manolache, S., Wong, A.C.L., Denes, F.S.: Plasma-enhanced deposition of silver nanoparticles onto polymer and metal surfaces for the generation of antimicrobial characteristics. *J. Appl. Polym. Sci.* **93**(3), 1411–1422 (2004)
2. Shankar, S.S., Rai, A., Ahmad, A., Sastry, M.: Rapid synthesis of Au, Ag, and bimetallic Au core–Ag shell nanoparticles using neem (*Azadirachta indica*) leaf broth. *J. Colloid Interface Sci.* **275**(2), 496–502 (2004a)

3. Chandran, S.P., Chaudhary, M., Pasricha, R., Ahmad, A., Sastry, M.: Synthesis of gold nanotriangles and silver nanoparticles using Aloe vera plant extract. *Biotechnol. Prog.* **22**(2), 577–583 (2006)
4. Li, S., Shen, Y. Xie., A. Yu, X., Qiu, L., Zhang, L., Zhang, Q.: Green synthesis of silver nanoparticles using capsicum annum L. extract. *Green Chem.* **9**(8), 852–858 (2007)
5. Leela, A., Vivekanandan, M.: Tapping the unexploited plant resources for the synthesis of silver nanoparticles. *Afr. J. Biotechnol.* **7**(17), 3162–3165 (2008)
6. Jain, N., Bhargava, A., Majumdar, S., Panwar, J.: Extracellular biosynthesis and characterization of silver nanoparticles using *Aspergillus flavus* NJP08: a mechanism prospective. *Nanoscale* **3**(2), 635–641 (2011)
7. Begum, N.A., Mondal, S., Basu, S., Laskar, R.A., Mandal, D.: Biogenic synthesis of Au and Ag nanoparticles using aqueous solution of black tea leaf extracts. *Colloids Surf B* **71**(1), 113–118 (2009)
8. Bar, H., Bhui, D.K., Sahoo, G.P., Sarkar, P., Pyne, S., Misra, A.: Green synthesis of silver nanoparticles using seed extract of *Jatropha curcas*. *Colloids Surf A* **348**(1), 212–216 (2009)
9. Dubey, M., Bhadauria, S., Kushwah, B.S.: Green synthesis of nanosilver particles from extract of *Eucalyptus hybrida* (Safeda) leaf. *Dig. J. Nanomaterials Biostructures* **4**(3), 537–543 (2009)
10. El-Naggar, N.E., Abdelwahed, N.A.M., Darwesh, O.M.M.: Fabrication of biogenic antimicrobial silver nanoparticles by streptomyces aegyptia NEAE 102 as eco-friendly nanofactory. *J. Microbiol. Biotechnol.* **24**(4), 453–464 (2014). <http://dx.doi.org/10.4014/jmb.1310.10095>
11. Prabhu, Y.T., Rao, K.V., Sai, V.S., Pavani, T.: A facile biosynthesis of copper nanoparticles: a micro-structural and antibacterial activity investigation. *J. Saudi Chem. Soc.* (2015). <http://dx.doi.org/10.1016/j.jscs.2015.04.002>
12. Kale, R., Kane, P.: Colour removal using nanoparticles. *Text. Clothing Sustain.* **2**(1), 1–7 (2016)
13. Kale, R., Kane, P., Phulaware, N.: Decolourization of C. I. reactive black 5 by PVP stabilized nickel nanoparticles. *Int. J. Eng. Sci. Innovative Technol.* **3**(2) (2014)

Advances in Health and Environment Safety

Select Proceedings of HSFEA 2016

Siddiqui, N.A.; Tauseef, S.M.; Bansal, K. (Eds.)

2018, XVIII, 396 p. 120 illus., 103 illus. in color.,

Hardcover

ISBN: 978-981-10-7121-8